Trajectory-Based Stabilization of Periodic Orbits*

Niklas Kruse†, Wolfram Just†, and Jens Starke†

Abstract. We present a data-driven feedback control scheme, which stabilizes unstable periodic orbits of dynamical systems. Model equations of the underlying system are assumed to be unavailable. Our approach relies only on previously measured input-state trajectories of a Poincaré map of the system. The success of a stabilizing feedback control in experimental systems typically depends on an adequate choice of control gains. The presented scheme computes stabilizing control gains by solving an optimization problem. No explicit model is identified and the control gains are computed directly from the measured trajectories. As a demonstration, we apply the scheme to a control-based continuation problem and obtain the corresponding bifurcation diagram.

Key words. data-driven control, Poincaré map, periodic orbit, control-based continuation

MSC codes. 37N35, 34H05, 34H20

1. Introduction.

Experimental systems typically depend on parameters, which can be adjusted in order to obtain a desired behavior. This desired behavior may be represented by a stationary state or some periodic solution in the state space. If these are unstable, meaning that initialization near but not exactly at them causes the system state to diverge, the desired behavior is not observable in the experiment, which never allows for exact initialization. Even if one succeeds at initializing the experiment exactly at for example an unstable stationary state, the never completely avoidable external disturbances would again cause the system state to diverge. To overcome this, feedback control is often used for the stabilization of an unstable steady state of the underlying system [22, 26, 12, 29]. When the desired behavior is represented by a certain unstable periodic solution in the state space, one can again rely on feedback control, to stabilize these periodic orbits and thus making them observable in the corresponding experiment. One way to extend linear feedback control to this scenario was suggested in [27]. The idea is to reduce the stabilization of the desired periodic solution to the stabilization of the corresponding fixed point of a Poincaré map [19]. Consequently, feedback control techniques for stabilizing fixed points of discrete-time systems can be applied. But, having the application of these techniques in real experiments in mind, we want to point out the following two problems.

Feedback control is often formulated in a framework, which assumes that the experimental system is modeled by a system of differential equations. While in some situations, first principles allow for deriving such an analytic model, this is not always the case. To overcome this, data-based control strategies are used [32, 24]. These are based on a data-driven identification of a linear control system, which are amenable for linear feedback control [26, 12]. Furthermore, we want to point out that feedback control relies on an adequate choice of control gain

*Submitted to the editors DATE.

Funding: Financial support by the German Research Foundation (Deutsche Forschungsgemeinschaft, DFG) – SFB 1270/2 - 299150580 is greatly acknowledged.

†Institute of Mathematics, University of Rostock, Ulmenstraße 69, 18057 Rostock, Germany (niklas.kruse@uni-rostock.de, wolfram.just@uni-rostock.de, jens.starke@uni-rostock.de).

parameters. Having an analytic model at hand, which was either derived or identified with the aid of the above mentioned data-based identification methods, there exists methods for computing stabilizing control gains [26, 12]. Also, model-based methods for designing feedback control laws of nonlinear systems are available, which include for example linearization via feedback, sliding mode control, backstepping and passivity-based control [22, 23]. However, motivated by the fact that experimental systems are naturally observed through time series of some number of measurement variables, it was shown in [14, 13, 6, 2], that one can directly compute stabilizing control gains from collected time series. This means, that a model identification is not required, which sometimes is referred to as a trajectory-based approach. These trajectory-based methods are used to stabilize known fixed points of discrete- and continuous-time control systems and have also been used in a model predictive control scheme [7]. In this work, we extend this framework to the stabilization of periodic orbits of continuous-time systems. In [9], the above mentioned model identification methods were used, to derive analytic expressions of Poincaré maps, which allows for stabilizing unstable periodic orbits via linear feedback control. Although we ultimately have the same goal, our approach is not based on this explicit model identification and computes stabilizing control gains directly from observed time series of a Poincaré map. We apply the proposed scheme by tracking an unstable branch of periodic orbits, which appears in a system, that is defined from the normal form of the saddle-node bifurcation. This is referred to as control-based continuation [38, 36, 37, 4, 5, 11, 10, 35, 33, 3, 1, 30, 15, 31, 16, 8]. While some of the mentioned articles already use feedback control for stabilizing unstable steady states or periodic orbits in laboratory experiments, finding adequate control gains remains a challenging problem. With the proposed scheme, we are taking a step towards a systematic calculation of control gains.

The remainder of this article is structured as follows. In section 2, we give an overview of trajectory-based data-driven feedback control of discrete-time systems. Section 3 includes an extension to the stabilization of unstable periodic orbits of continuous-time systems via a Poincaré map. We embed the proposed method into an integral control setup, which is used to solve a control-based continuation problem. Section 4 concludes this article.

2. Data-driven feedback control of discrete-time systems.

Trajectory-based control methods allow for constructing stabilizing feedback controllers without having to identify an explicit model. Instead, an input-state time series of the given system is recorded. Subsequently, stabilizing control gains are computed by solving an optimization problem with convex constraints. This method is based on data-driven linear control theory, to which we now turn.

2.1. Trajectory-based methods for linear systems.

First, we review some of the results that are included in [14, 32]. For given matrices $A \in \mathbb{R}^{N\times N}$ and $B \in \mathbb{R}^N$, consider a discrete-time linear system

$$x_{n+1} = Ax_n + Bu_n, \tag{2.1}$$

where $x_n \in \mathbb{R}^N$ denotes the state and $u_n \in \mathbb{R}$ refers to a control parameter at time n.

Choosing an initial state x_0 and a sequence $u_0, u_1, \dots, u_{T-1}$ of $T > 0$ control parameter values, we compute via (2.1) a corresponding sequence $x_0, x_1, \dots, x_T$ of states. The first

question is, whether it is possible to compute A and B only from the obtained simulation data

$$\begin{aligned} U &= \begin{bmatrix} u_0 & u_1 & \dots & u_{T-1} \end{bmatrix} \\ X &= \begin{bmatrix} x_0 & x_1 & \dots & x_{T-1} \end{bmatrix} \\ Y &= \begin{bmatrix} x_1 & x_2 & \dots & x_T \end{bmatrix}. \end{aligned} \tag{2.2}$$

This is answered by

Theorem 2.1 ([14]). *Suppose that*

$$\operatorname{rank} \begin{bmatrix} U \\ X \end{bmatrix} = N + 1.$$

Then, it follows that

$$\begin{bmatrix} B & A \end{bmatrix} = Y \begin{bmatrix} U \\ X \end{bmatrix}^{\dagger}.$$

where

$$\begin{bmatrix} U \\ X \end{bmatrix}^{\dagger} = \begin{bmatrix} U^T & X^T \end{bmatrix} \left(\begin{bmatrix} U \\ X \end{bmatrix} \begin{bmatrix} U^T & X^T \end{bmatrix} \right)^{-1}$$

denotes the right inverse, which exists due to the rank condition.

In the general case, starting with experimentally obtained data of the form (2.2), one is interested in solving the least squares problem

$$\min_{C} \left\| Y - C \begin{bmatrix} U \\ X \end{bmatrix} \right\|_F, \tag{2.3}$$

where $\|Z\|_F = \sqrt{\sum_{i,j} |z_{ij}|^2}$ denotes the Frobenius norm. Note that the square of the Frobenius norm is a quadratic function in the absolute values of the matrix elements and therefore the minimization leads to a linear zero problem. If the rank condition of Theorem 2.1 holds, it follows that

$$C = Y \begin{bmatrix} U \\ X \end{bmatrix}^{\dagger}$$

is the unique minimizer of (2.3), where $\begin{bmatrix} U \\ X \end{bmatrix}^{\dagger}$ denotes the right inverse from Theorem 2.1. Defining matrices $A \in \mathbb{R}^{N \times N}$ and $B \in \mathbb{R}^{N}$ by setting

$$\begin{bmatrix} B & A \end{bmatrix} = Y \begin{bmatrix} U \\ X \end{bmatrix}^{\dagger}$$

gives a linear approximation $x_{n+1} \approx Ax_n + Bu_n$ of the experimental system subject to control inputs. This identification method is referred to as dynamic mode decomposition with control [32].

If the matrix $C = \begin{bmatrix} B & AB & \dots & A^{N-1}B \end{bmatrix}$ has full rank, the linear system of the form (2.1) is called controllable. It follows from this, that one can compute a matrix $K \in \mathbb{R}^{1\times N}$, such that the eigenvalues of the matrix $A + BK$ lie at predetermined locations. In particular, one can place all eigenvalues inside the unit circle. If this is the case, we say that the controller $u_n = Kx_n$ is stabilizing. This is equivalent to the fact, that the trajectories of the closed-loop system

$$x_{n+1} = (A + BK)x_n \tag{2.4}$$

converge to the origin for every initial condition, see e.g. [26]. Thus, after identification of a controllable linear system from data, one can design a stabilizing feedback controller. While for given matrices A and B there exist efficient algorithms for doing so, we aim for a stabilizing feedback control, which is computable directly from the data (2.2). This means, no explicit model is given nor it has to be identified during the application of the method. A key result in this direction is given by

Theorem 2.2 ([14]). *Consider the discrete-time linear system (2.1). Suppose that*

$$\operatorname{rank} \begin{bmatrix} U \\ X \end{bmatrix} = N + 1. \tag{2.5}$$

Then, for a given $K \in \mathbb{R}^{1\times N}$, there exists a $G \in \mathbb{R}^{T\times N}$ with

$$\begin{bmatrix} K \\ I \end{bmatrix} = \begin{bmatrix} U \\ X \end{bmatrix} G$$

and

$$A + BK = YG,$$

where I denotes the $N \times N$ identity matrix.

Conversely, if (2.5) holds, choosing a $G \in \mathbb{R}^{T\times N}$ with $I = XG$ and setting $u_n = UGx_n$ implies the closed loop representation

$$A + BUG = YG.$$

Note that the first part of Theorem 2.2 provides for a fixed control gain matrix K a way of computing the matrix $A+BK$ of the closed-loop system (2.4) directly from the data (2.2). This makes it possible to check whether for a given K, the feedback control $u_n = Kx_n$ is stabilizing. On the other hand, due to the second part, one can search for a G with $I = XG$, such that the feedback control $u_n = UGx_n$ becomes stabilizing without an explicit identification of A and B. This forms the basis of

Theorem 2.3 ([14]). *Suppose that*

$$\operatorname{rank} \begin{bmatrix} U \\ X \end{bmatrix} = N + 1. \tag{2.6}$$

Then, given a matrix $Q \in \mathbb{R}^{T \times N}$ such that XQ is symmetric and

$$\begin{bmatrix} XQ & YQ \\ Q^T Y^T & XQ \end{bmatrix} \tag{2.7}$$

is positive definite, the matrix $(XQ)^{-1}$ exists and the feedback controller $u_n = Kx_n$ with

$$K = UQ(XQ)^{-1} \tag{2.8}$$

is stabilizing.

Conversely, if (2.6) holds and K is stabilizing, then there exists a Q such that (2.7) is positive definite and (2.8) holds.

Thus, as long as the rank condition is satisfied, the second part of Theorem 2.3 parametrizes all stabilizing gain matrices K by the data matrices (2.2), that are obtained from computing one input-state trajectory of the system (2.1). If, in addition, the system is controllable, it follows that there exists at least one solution Q with the desired properties. In fact, finding a Q that renders (2.7) positive definite can be cast as a standard problem in the framework of linear matrix inequalities, see e.g. [34]. Linear matrix inequalities are convex constraints and thus the stated problem is convex. For a numerical computation of the matrix Q, efficient solvers such as CVX are available [18, 17].

2.2. Extension to nonlinear systems via nonlinearity cancellation. One can extend the previous considerations of linear control theory to certain classes of nonlinear systems. So far, we have seen that designing a stabilizing controller for a linear system of the form (2.1) does not require an a priori identification of the matrices A and B. Although there exists a direct extension of this idea to the case of nonlinear systems, it is restricted in the following sense. While a controller, which renders the linearization around an equilibrium point of a given nonlinear system stable, also locally stabilizes the nonlinear system, there is no further information on the basin of attraction of the stabilized point. In practice, one might have to initialize the system extremely close to the point to be stabilized, which is not always possible. To circumvent this, trajectory-based feedback linearization can be used [13, 23, 21, 25]. The key idea of this concept can be explained as follows.

Consider the control system

$$x_{n+1} = x_n - x_n^2 + u_n, \tag{2.9}$$

where $x_n \in \mathbb{R}$ and $u_n \in \mathbb{R}$. Observe that any feedback law $u_n = k_1 x_n + k_2 x_n^2$ with $|1 + k_1| < 1$ and $k_2 = 1$ globally stabilizes the origin. To see this, note that the closed-loop dynamics read

$$x_{n+1} = (1 + k_1) x_n.$$

Thus, $x_n \to 0$ for $n \to \infty$ regardless of the initial condition x_0.

Returning to the trajectory-based setup of the stated theorems, one would like to compute such a globally stabilizing $K = \begin{bmatrix} k_1 & k_2 \end{bmatrix}$ directly from data. For a special class of nonlinear systems, this is indeed possible. We restrict ourselves to systems of the form

$$x_{n+1} = Ag(x_n) + Bu_n. \tag{2.10}$$

Here, x_n, u_n and B are as in (2.1), while $A \in \mathbb{R}^{N \times R}$. The nonlinearities are included in the map $g : \mathbb{R}^N \to \mathbb{R}^R$, which is assumed to be continuous. For example, the system (2.9) is of this form with

$$A = \begin{bmatrix} 1 & -1 \end{bmatrix}$$
$$B = 1$$
$$g(x) = \begin{bmatrix} x \\ x^2 \end{bmatrix}$$

and $R = 2$. For the purpose of illustration, we assume here that we know a continuous function $h : \mathbb{R}^N \to \mathbb{R}^S$ such that

$$g(x) = Ch(x) \tag{2.11}$$

for some matrix $C \in \mathbb{R}^{R \times S}$, where $S \geq N$. Later we will show that in applications such an assumption may not be required. In the following, we review some of the results obtained in [13]. For this, we compute data matrices of the form (2.2) via (2.10) for a fixed initial condition x_0 and a chosen sequence $u_0, u_1, \ldots, u_{T-1}$ of control parameter values, but also include $h(x_0), h(x_1), \ldots, h(x_{T-1})$. This results in the data set

$$\begin{aligned} U &= \begin{bmatrix} u_0 & u_1 & \ldots & u_{T-1} \end{bmatrix} \\ X &= \begin{bmatrix} x_0 & x_1 & \ldots & x_{T-1} \end{bmatrix} \\ Y &= \begin{bmatrix} x_1 & x_2 & \ldots & x_T \end{bmatrix} \\ H &= \begin{bmatrix} h(x_0) & h(x_1) & \ldots & h(x_{T-1}) \end{bmatrix}. \end{aligned} \tag{2.12}$$

Corresponding to Theorem 2.3, one has

Theorem 2.4 ([13]). *Suppose that*

$$\operatorname{rank} \begin{bmatrix} U \\ H \end{bmatrix} = S + 1. \tag{2.13}$$

If there exist matrices $P = P^T \in \mathbb{R}^{N \times N}$, $Z \in \mathbb{R}^{T \times N}$ and $G \in \mathbb{R}^{T \times (S-N)}$ such that

$$\begin{aligned} HZ &= \begin{bmatrix} P \\ 0_{(S-N) \times N} \end{bmatrix} \\ &\begin{bmatrix} P & (YZ)^T \\ YZ & P \end{bmatrix} \text{ is positive definite} \\ HG &= \begin{bmatrix} 0_{N \times (S-N)} \\ I_{S-N} \end{bmatrix} \\ YG &= 0_{N \times (S-N)} \end{aligned} \tag{2.14}$$

holds, then the control law $u_n = Kh(x_n)$*, where*

$$K = U \begin{bmatrix} ZP^{-1} & G \end{bmatrix}, \tag{2.15}$$

implies closed-loop dynamics of the form

$$x_{n+1} = Dx_n, \tag{2.16}$$

such that all eigenvalues of D *have absolute value less than one. Here,* $0_{k\times l}$ *denotes the zero matrix of dimension* $k \times l$ *and* I_k *is the* $k \times k$ *identity matrix.*

Conversely, if (2.13) holds and there exists a stabilizing K*, such that the closed loop dynamics are of the form (2.16), then* K *can be written as in (2.15) for some* P, Z, G *satisfying (2.14).*

Note that, in contrast to [13], we have slightly adjusted the notation for our purposes. Theorem 2.4 gives a way of designing globally stabilizing control laws for a specific class of nonlinear system. There is no systems identification step involved and the control gains are computed directly from the data (2.12). However, for some systems of the form (2.10), a fully linearizing controller does not exist. In this case, the convex program of Theorem 2.4 can be recast as a minimization problem. In this way, one obtains a controller, that minimizes the nonlinearities of the given system and locally stabilizes the origin, for details, see [13].

As an example, consider the map

$$\begin{aligned} x_{n+1} &= y_n \\ y_{n+1} &= -x_n + 3y_n - y_n^3 + u_n \end{aligned} \tag{2.17}$$

defined on the plane, which has been suggested as an approximation of the Poincaré map corresponding to the Duffing oscillator [20]. The origin is an unstable fixed point of the map for $u_n = 0$. The given system is of the form (2.10) with

$$\begin{aligned} A &= \begin{bmatrix} 0 & 1 & 0 \\ -1 & 3 & -1 \end{bmatrix} \\ g(x,y) &= \begin{bmatrix} x & y & y^3 \end{bmatrix}^T \\ B &= \begin{bmatrix} 0 \\ 1 \end{bmatrix}. \end{aligned}$$

We do not intend to use the information about the right-hand side of (2.17) for deriving a globally stabilizing control law. Instead we choose

$$h(x,y) = \begin{bmatrix} x & y & x^2 & xy & y^2 & x^3 & x^2y & xy^2 & y^3 \end{bmatrix}^T \tag{2.18}$$

as our library of basis functions. Note that with this choice, we include every function that appears in (2.17) and thus, equation (2.11) holds. In general, it is not possible to check this condition which makes the application of the described trajectory-based method somehow heuristic.

To compute a globally stabilizing control law via the convex program (2.14), we collect data matrices of the form (2.12). For this, we choose $x_0 = 0$ and $y_0 = 0$ as an initial condition and define the control parameter values $u_0, u_1, \ldots, u_{14}$ to be uniformly distributed random numbers in the interval $(-0.025, 0.025)$. Note, that in this example $T = 15$ and $S = 9$ holds. Finally, we use CVX to solve the convex program (2.14). From the obtained solution we compute a gain matrix $K = \begin{bmatrix} 0.94 & -2.42 & 0 & 0 & 0 & 0 & 0 & 0 & 1.00 \end{bmatrix}$ by using equation (2.15). We define the feedback control $u_n = Kh(x_n, y_n)$ and insert it into the system (2.17). A simulation with $x_0 = 2$ and $y_0 = -2$ results in the time series shown in Figure 1. The time series of the state components is shown in Figure 1a, while Figure 1b displays the control signal over time. Both state components as well as the control signal rapidly converge to zero.

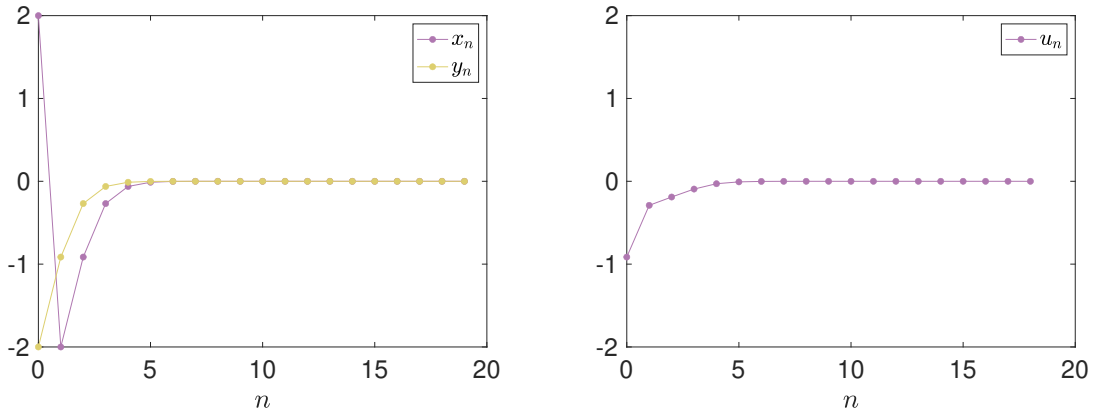

Figure 1: Simulated time series of the system (2.17) for the initial condition $(x_0, y_0) = (2, -2)$. The control signal is set to $u_n = Kh(x_n, y_n)$, where K is obtained from the solution of the convex program (2.14) and h is as in (2.18). (a) Time series of the state components. (b) Time series of the feedback control signal.

To illustrate the global stability of the origin under the constructed feedback control, we numerically compute its basin of attraction. By this we mean the set of initial conditions, that lead to convergence of both state components to zero after a sufficiently long simulation time. A part of this basin is shown in Figure 2a. For comparison, Figure 2b shows a part of a basin, that is obtained by simulating the system (2.17) subject to linear feedback control of the form $u_n = k_1 x_n + k_2 y_n$. Here, the control gains k_1 and k_2 are chosen in such a way, that the linearization of the system (2.17) at the origin has only eigenvalues with absolute value less than one. Note that, since the chosen h given in (2.18) contains all the functions that appear in the system (2.17), Theorem 2.4 guarantees global stability of the origin.

This example shows, that by solving the convex program (2.14), one may be able to construct a globally stabilizing control for certain classes of nonlinear systems. Furthermore, no explicit model is needed and the controller is derived solely from the data matrices (2.12).

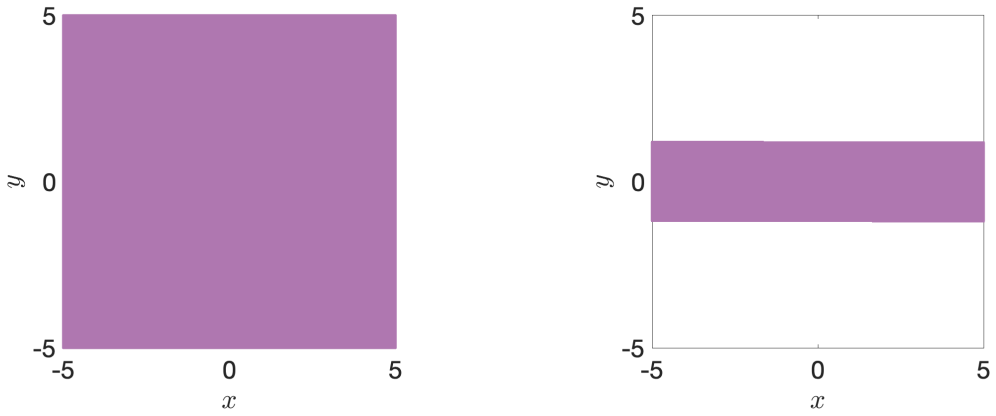

Figure 2: Numerically computed parts of the basins of attraction of the origin. These are computed by simulating the closed-loop dynamics of the system (2.17) for nonlinear as well as linear feedback control. (a) The control signal is set to $u_n = Kh(x_n, y_n)$, where K is obtained from the solution of the convex program (2.14) and h is as in (2.18). (b) The control signal is set to $u_n = k_1 x_n + k_2 y_n$. Here, k_1 and k_2 are chosen in such a way, that the linearization of the system (2.17) at the origin has only eigenvalues with absolute value less than one.

These are generated by one input-state trajectory of the given system as well as some suitable choice of the function h. However, so far we have only discussed the stabilization of the origin. In control-based continuation problems also nonzero fixed points are to be stabilized. Taking this into account, one has to modify the control law. This is explained in the following section.

3. Application to control-based continuation. So far we have demonstrated how to design globally stable control schemes for unstable fixed points based on plain time series. We now address the question of how to use such ideas for system analysis, in particular, how to track unstable states and how to uncover bifurcation scenarios when just plain time series are at hand.

3.1. Trajectory-based tracking of unstable states. To explain the main ideas we use a simple normal form for the purpose of illustration. Consider again the one-dimensional control system

$$x_{n+1} = x_n - x_n^2 + u_n = f(x_n, u_n). \tag{3.1}$$

For a fixed value of u_n, the map $f(\cdot, u_n)$ can have multiple fixed points. In fact, if $\bar{u}$ denotes a constant parameter value, the fixed points are given as the real solutions of the equation $\bar{x}^2 = \bar{u}$. Thus, for a negative $\bar{u}$ there exists no real fixed point, while for $\bar{u} \geq 0$ we have the fixed points $\sqrt{\bar{u}}$ and $-\sqrt{\bar{u}}$, which coalesce for $\bar{u} = 0$. Furthermore, by inspecting the linearization of the map for $0 < \bar{u} < 1$, it follows that the fixed points $\sqrt{\bar{u}}$ are asymptotically stable, while the points $-\sqrt{\bar{u}}$ are unstable. One therefore refers to the graph of the function $\sqrt{\bar{u}}$ over the

interval $0 < \bar{u} < 1$ as the stable branch. The graph of $-\sqrt{\bar{u}}$ over the same interval is the unstable branch. These two branches are connected by the bifurcation point $(\bar{u}, \bar{x}) = (0, 0)$. This bifurcation analysis is also possible for a more general class of parameter-dependent maps and differential equations [19].

Control-based continuation now aims for the following. If the control system is initialized for a fixed parameter value in a sufficiently small neighborhood of a stable branch, the state is converging to the corresponding stable fixed point on the branch. Subsequently, a nearby point $(\bar{u}, \bar{x})$ on the branch is selected by the continuation scheme and the controller acts, such that both the state as well as the parameter converge to the selected coordinates $(\bar{u}, \bar{x})$. This is repeated until sufficiently many points on the stable as well as on the unstable branches are stabilized. This detects a part of a complete bifurcation diagram of the given system. In experimental system, model equations are not always accessible. Consequently, there is no a priori information about the location of the branches. Nevertheless, the attraction of the stable branch makes it possible to locate a point on it by initialization. This can then be used as a starting point for a continuation scheme. In the following, the trajectory-based controller of Section 2 is modified, so that it drives the system along its stable and unstable branches. Given the fact, that the framework of Section 2 is purely data-driven, model equations are not required and control gains are computed directly from an input-state trajectory of the system.

The suggested method is illustrated by the example (3.1), which serves to illustrate the effect of including a reference value directly into the control law under the assumption that we already obtained a stabilizing controller for the given system. The solution of the convex program (2.14) leads to a controller $u_n = kx_n + x_n^2$, such that in closed-loop we have $x_{n+1} = (1 + k)x_n$. Here, $|1 + k| < 1$ holds, so the controller globally stabilizes the origin. Including a reference parameter r in the control law, yields $u_n = r + kx_n + x_n^2$ and

$$x_{n+1} = (1 + k)x_n + r.$$

The explicit solution of this system is given by

$$x_n = (1 + k)^n x_0 + r \sum_{i=0}^{n-1} (1 + k)^i, \quad n \geq 0.$$

Consequently, the modified controller globally stabilizes a fixed point $\bar{x}$ that is given by

$$\bar{x} = \lim_{n\to\infty} x_n = r \left(\frac{1}{1 - (1 + k)} \right) = r \left(\frac{1}{-k} \right). \tag{3.2}$$

Furthermore, the control parameter converges to

$$\bar{u} = \lim_{n\to\infty} u_n = r + k\bar{x} + \bar{x}^2 = r + kr \left(\frac{1}{-k} \right) + \bar{x}^2 = \bar{x}^2.$$

Thus, for a fixed nonzero value of the reference r, the system is driven to some point $(\bar{u}, \bar{x})$ on the stable or unstable branch. If one chooses $r = 0$, the system converges to the bifurcation point $(\bar{u}, \bar{x}) = (0, 0)$. Also, note that $|1 + k| < 1$ implies $-2 < k < 0$. Consequently, the

relation between the reference and the stabilized fixed point is given by $\bar{x} = rc$ for some positive constant c. For the special case $k = -1$, the selected reference equals the stabilized fixed point. By using different reference values, sufficiently many points on the branches can be stabilized and a part of the full bifurcation diagram becomes visible. We further point out, that the controller is computed solely from an input-state time series of the system. Finally, if a full nonlinearity cancellation is possible, the controller globally stabilizes the fixed points and a nearby initialization is not necessary. This differs from the control-based continuation methods, that are based on linear feedback control, where only local stabilization is achieved.

Figure 3 shows a set of stabilized points on the stable as well as on the unstable branch of example (3.1). These are generated by using the presented continuation scheme. The controller is obtained by numerically solving the convex program (2.14) for a recorded input-state trajectory of the system (3.1). For details of how to generate such a trajectory, we refer to example (2.17) of section 2. The function h is set to $h(x) = \begin{bmatrix} x & x^2 & x^3 & x^4 & x^5 \end{bmatrix}^T$. In order to drive the system to different points on the branches, we vary the reference r in the control law.

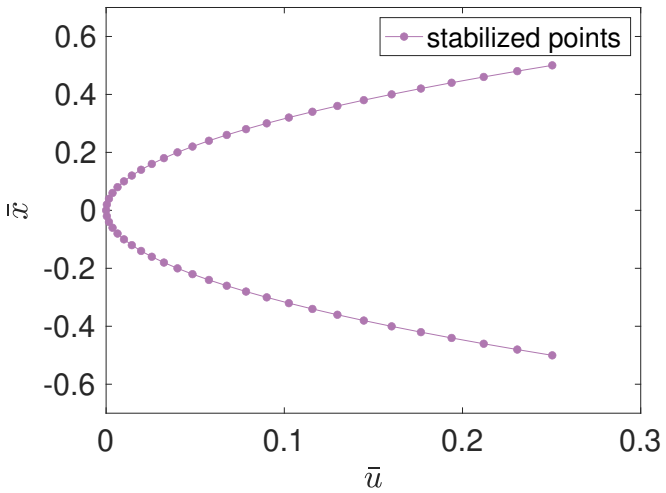

Figure 3: Bifurcation diagram with parameter $\bar{u}$: A set of stabilized points on the stable and unstable branch of the system (3.1). Here, the controller $u_n = Kh(x_n) + r$ is used, where K is obtained from the solution of the convex program (2.14). The function h is defined as $h(x) = \begin{bmatrix} x & x^2 & x^3 & x^4 & x^5 \end{bmatrix}^T$. In order to drive the system to different points on the branches, the reference r is varied.

As was already pointed out, if a full nonlinearity cancellation is possible, the controller globally stabilizes the points on the branches. Continuation schemes, that are based on linear feedback control, generally do not have this property and may depend on an initialization near the point to be stabilized. The global property can be utilized in the following situation. Suppose an experimental system has to abruptly change its state from one point on the stable branch to some point on the unstable branch, in order to maintain some optimality property

[27]. The presented control scheme is able to meet such a requirement, without having to assume that the points lie in a small neighborhood. Figure 4 illustrates a fast switching from one point on the stable branch of the system (3.1) to one point of its unstable branch.

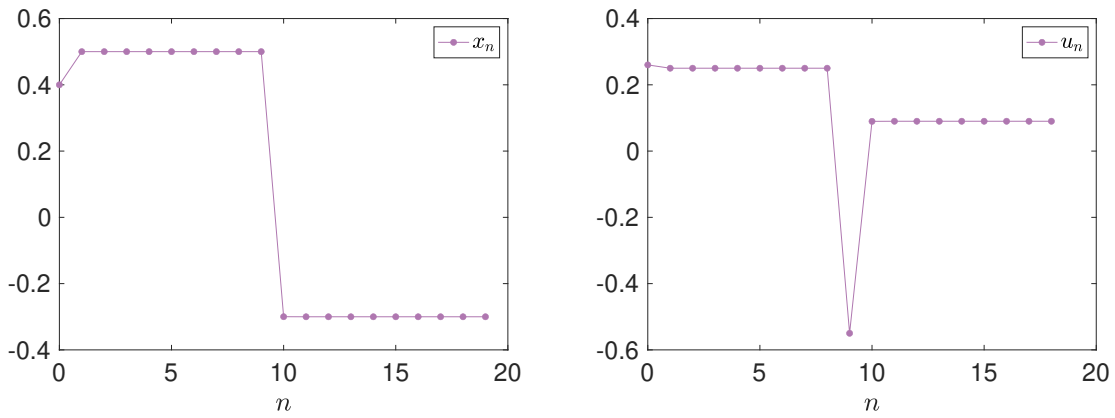

(a) (b)

Figure 4: Simulated time series of the system (3.1) for the initial condition $x_0 = 0.4$. The control signal is set to $u_n = Kh(x_n) + r$, where K is obtained from the solution of the convex program (2.14) and the function h is defined as $h(x) = \begin{bmatrix} x & x^2 & x^3 & x^4 & x^5 \end{bmatrix}^T$. For $0 \leq n \leq 8$, the reference is set to $r = 0.5$, while for $9 \leq n \leq 18$ we choose $r = -0.3$. This induces a fast switching from the fixed point 0.5 on the stable branch to the fixed point -0.3 on the unstable branch. (a) Time series of the state. (b) Time series of the feedback control signal.

3.2. Trajectory-based tracking of unstable periodic orbits with nonlinear integral control. In the following, we apply Theorem 2.4 or the mentioned minimization problem to discrete-time control systems, that are induced by parameter-dependent Poincaré maps. Continuous-time control systems of the form

$$\dot{x} = f(x, u), \tag{3.3}$$

where $x \in \mathbb{R}^N$ denotes the state and $u \in \mathbb{R}$ denotes the control parameter, can have periodic solutions [19]. These are characterized by the property, that there exists a real $T > 0$ such that $\phi(t) = \phi(t + T)$ and $\phi(t) \neq \phi(t + \tau)$ for all real τ with $0 < \tau < T$. Here, ϕ denotes the solution curve of (3.3) through a fixed initial condition and control parameter equal to zero. Such a periodic orbit γ induces a parameter-dependent Poincaré map as follows. First, we construct an $(N-1)$-dimensional hypersurface Σ, which is everywhere transversely intersected by the solution curves of the vector field $f(\cdot, 0)$. We assume, that γ intersects Σ at a unique point p. If γ intersects Σ at multiple points, than one can shrink Σ until there is only one intersection. Finally, we define a parameter-dependent Poincare map on a neighborhood U around $(x_n, u_n) = (p, 0)$ as

$$x_{n+1} = P(x_n, u_n), \tag{3.4}$$

where x_{n+1} denotes the first intersection of Σ by the solution curve of $f(\cdot, u_n)$, that is initialized at $x_n \in \Sigma$. Note that

$$P(p, 0) = p.$$

and thus, p is a fixed point of the map $P(\cdot, 0)$. The stability of the fixed point p characterizes the stability of the periodic orbit γ. Consequently, if the system (3.4) is of the form (2.10), we can use trajectory-based feedback linearization in order to stabilize γ.

In the following, we propose a trajectory-based control scheme, such that the prescribed reference r equals the stabilized fixed point $\bar{x}$. Note that for a fully linearizing controller $u_n = Kh(x_n) + r$ in a system like (3.1), equation (3.2) holds. Consequently, apart from the special case $k = -1$, the reference differs from the actual fixed point that is stabilized. To circumvent this problem, integral control can be used [26]. We will explain in the following how it can be used in a trajectory-based manner.

The method relies on the construction of an integrator state v_n, that sums up the deviation between the system state x_n and the reference r over time. In order to take this into account, the state equations of v_n are defined as

$$v_{n+1} = v_n + r - x_{n+1} = v_n + r - P(x_n, u_n), \qquad x_n, v_n, r \in \mathbb{R}^N,\ u_n \in \mathbb{R} \tag{3.5}$$

where $P(x_n, u_n)$ denotes a parameter-dependent Poincaré map. Then, the dynamics of the extended state (x_n, v_n) are governed by the system

$$\begin{aligned} x_{n+1} &= P(x_n, u_n) \\ v_{n+1} &= v_n + r - P(x_n, u_n). \end{aligned} \tag{3.6}$$

Assume, that for the system (3.6) with $r = 0$, a fully linearizing controller $u_n = Kh(x_n, v_n)$ can be constructed by solving the convex program (2.14). This yields the closed loop system

$$\begin{bmatrix} x_{n+1} \\ v_{n+1} \end{bmatrix} = A \begin{bmatrix} x_n \\ v_n \end{bmatrix},$$

such that all eigenvalues of the matrix A have absolute value less than one. Using the constructed controller in the system (3.6) for some nonzero reference r, yields

$$\begin{bmatrix} x_{n+1} \\ v_{n+1} \end{bmatrix} = A \begin{bmatrix} x_n \\ v_n \end{bmatrix} + \begin{bmatrix} 0 \\ I_N \end{bmatrix} r,$$

where $0 \in \mathbb{R}^{N \times N}$ denotes the zero matrix and $I_N \in \mathbb{R}^{N \times N}$ the identity matrix. The given system converges to

$$\begin{aligned} \begin{bmatrix} \bar{x} \\ \bar{v} \end{bmatrix} &= \lim_{n \to \infty} \begin{bmatrix} x_n \\ v_n \end{bmatrix} = \lim_{n \to \infty} \left(A^n \begin{bmatrix} x_0 \\ v_0 \end{bmatrix} \right) + \left(\lim_{n \to \infty} \sum_{i=0}^{n-1} A^i \right) \begin{bmatrix} 0 \\ I_N \end{bmatrix} r \\ &= \left(\lim_{n \to \infty} \sum_{i=0}^{n-1} A^i \right) \begin{bmatrix} 0 \\ I_N \end{bmatrix} r = (I_{2N} - A)^{-1} \begin{bmatrix} 0 \\ I_N \end{bmatrix} r \end{aligned}$$

for every initial condition (x_0, v_0). Furthermore, the control signal converges to

$$\bar{u} = \lim_{n\to\infty} u_n = Kh(\bar{x}, \bar{v}).$$

Finally, the point $\bar{x}$ is a fixed point of the map $P(\cdot, \bar{u})$ since

$$\bar{x} = \lim_{n\to\infty} x_{n+1} = P(\bar{x}, \bar{u}).$$

But, by equation (3.5), we have $\bar{v} = \bar{v} + r - \bar{x}$, which implies that $\bar{x} = r$.

For an illustration of the presented control scheme, consider the differential equation

$$\begin{aligned} \dot{x} &= 10y + \frac{x\left(u - x^2 - y^2 - 1 + 2\sqrt{x^2+y^2}\right)}{\sqrt{x^2+y^2}} \\ \dot{y} &= -10x + \frac{y\left(u - x^2 - y^2 - 1 + 2\sqrt{x^2+y^2}\right)}{\sqrt{x^2+y^2}} \end{aligned} \tag{3.7}$$

defined on $\mathbb{R}^2 \setminus \{0\}$. Here, $u \in \mathbb{R}$ denotes the control parameter. A one-dimensional hypersurface Σ is defined as $\Sigma = \{(x, y) : x > 0, y = 0\}$. Given a point $(x_n, 0) \in \Sigma$ and a fixed value u_n of the control parameter, we numerically integrate the differential equation until the orbit of the given vector field intersects Σ again. Denoting the point of intersection by $(x_{n+1}, 0) \in \Sigma$, we obtain a one-dimensional parameter-dependent Poincaré map $x_{n+1} = P(x_n, u_n)$. Note that in this example, no analytical expression for the map P is given. By transforming the system (3.7) to polar coordinates, it can be shown that for a given positive value of u, there exists a stable as well as an unstable periodic orbit. In fact, qualitatively, the bifurcation diagram of the map P looks the same as the one depicted in Figure 3, where the upper branch corresponds to stable periodic orbits and the lower branch corresponds to the unstable ones. Our aim is to reconstruct the bifurcation diagram of P by using the presented trajectory-based integral control scheme.

In the first step, the convex program (2.14) is solved for the extended system (3.6) with $r = 0$. For this, data of the form (2.12) is generated, where

$$h(x, v) = \begin{bmatrix} x & v & x^2 & xv & v^2 & x^3 & x^2v & xv^2 & v^3 \end{bmatrix}^T.$$

Finally, the obtained controller $u_n = Kh(x_n, v_n)$ with

$$K = \begin{bmatrix} -0.72 & 0.09 & 0.69 & 0 & 0 & -0.60 & 0 & 0 & 0 \end{bmatrix}$$

is used in the extended system (3.6) for different nonzero reference values r. By construction, the integral controller drives the state x_n to the selected reference. The control parameter converges to $\bar{u}$ such that $P(r, \bar{u}) = r$. A number of different stabilized points corresponding to different choices of the reference are shown in Figure 5. The described scheme is summarized in Algorithm 3.1.

To demonstrate the global stabilization property of the obtained controller, we again solve a switching problem from one point of the stable branch to one point of the unstable branch. Figure 6a shows the time series of the state as well as the reference signal and Figure 6b depicts the corresponding control signal. Observe that after changing the reference, the controller drives the state to the selected point on the unstable branch.

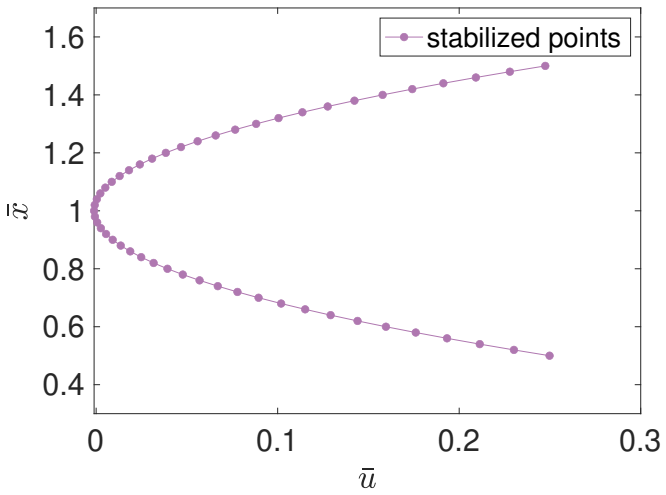

Figure 5: Bifurcation diagram with parameter $\bar{u}$: A set of stabilized points on the stable and unstable branch of the parameter-dependent Poincaré map corresponding to the system (3.7). Here, the controller $u_n = Kh(x_n, v_n)$ is used, where K is obtained from the solution of the convex program (2.14). The function h is defined as $h(x, v) = \begin{bmatrix} x & v & x^2 & xv & v^2 & x^3 & x^2v & xv^2 & v^3 \end{bmatrix}^T$. In order to drive the system to different points on the branches, the reference r is varied.

Algorithm 3.1 Trajectory-based stabilization of periodic orbits.

1: Construct a section to obtain a parameter-dependent Poincaré map.
2: Choose a function h, which contains the basis functions.
3: Generate data of the form (2.12) by simulating the extended system (3.6) for $r = 0$ and a chosen set of control parameter values.
4: Solve the convex program (2.14).
5: Compute the gain matrix K by using equation (2.15).
6: Use the obtained controller $u_n = Kh(x_n, v_n)$ in the extended system (3.6) for different nonzero reference values r in order to drive the system to different points on the branches.

4. Conclusions. Trajectory-based control methods allow for an automatic construction of a stabilizing controller based on one a priori recorded input-state trajectory. Section 2 shows that by utilizing feedback linearization, the linear setting can be extended to a class of nonlinear systems. Based on this extension, discrete-time control systems that are induced by parameter-dependent Poincaré maps are amenable to this method. As a result, unstable periodic orbits can be stabilized by the constructed controller, which is obtained by solving a convex program. This circumvents the problem of finding adequate control gains. Furthermore, in the case of a full nonlinearity cancellation, the controller globally stabilizes the unstable fixed point. Consequently, there is no need for a nearby initialization. The

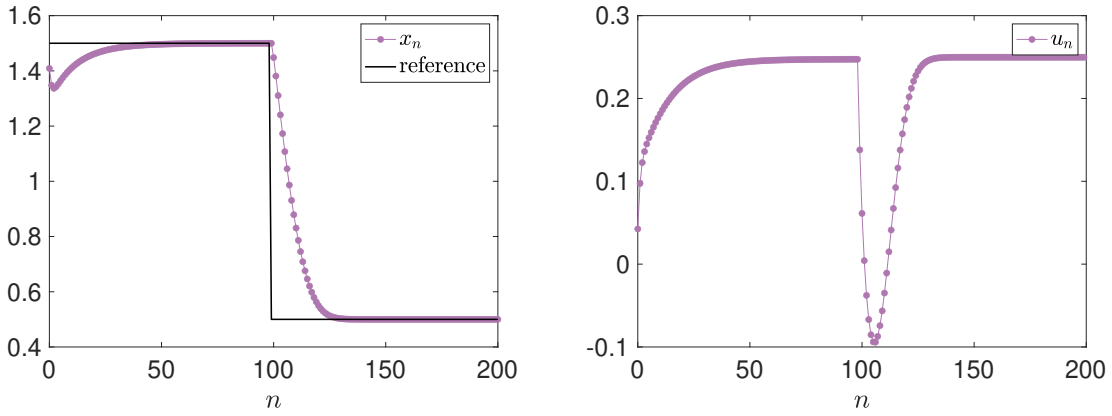

(a) (b)

Figure 6: Simulated time series of the Poincaré map corresponding to system (3.7). The control signal is set to $u_n = Kh(x_n, v_n)$, where K is obtained from the solution of the convex program (2.14). For $0 \leq n \leq 98$, the reference is set to $r = 1.5$, while for $99 \leq n \leq 200$ we choose $r = 0.5$. This induces a switching from the fixed point 1.5 on the stable branch to the fixed point 0.5 on the unstable branch. (a) Time series of the state together with the reference signal. (b) Time series of the feedback control signal.

embedding of the trajectory-based scheme into an integral control framework in section 3 allows for stabilization of nonzero fixed points, which makes it possible to use the method for control-based continuation problems. But, in contrast to continuation schemes that are based on linear feedback control, switching between a point on the stable branch to one on the unstable branch is possible without requiring the assumption that the points lie in a small neighborhood. Also, the robustness against external disturbances is increased by the global stabilization property, which is useful in an experimental setup.

There are several possible further research directions in this area. First, the proposed integral control scheme in section 3 assumes that the full state is available for feedback, which typically is not the case in experimental setups. Thus, either a state estimation scheme is needed or one would have to resort to output feedback, where the output includes all the measurement variables [26]. State estimation is possible by using delay coordinates [39, 28]. The influence of such modifications on the stabilization properties of the proposed method will be studied in the future. Furthermore, the presented method is not restricted to single-input systems. Thus, also Poincaré maps that depend on a multidimensional parameter can be handled. This could be used to discover more complex bifurcation diagrams. Also, periodically driven oscillators are amenable to the stabilization scheme. In fact, for this class of systems, it is possible to construct a globally defined Poincaré map, see e.g. [19]. Finally, a validation of the integral control scheme in a laboratory experiment would be useful and may lead to further research questions. For example, the influence of introducing delay into the integral

476 scheme on the stability could be studied.

477 REFERENCES

478 [1] G. Abeloos, L. Renson, C. Collette, and G. Kerschen, *Stepped and swept control-based continu-*
479 *ation using adaptive filtering*, Nonlinear Dynamics, 104 (2021), pp. 3793–3808.
480 [2] M. Alsalti, J. Berberich, V. G. Lopez, F. Allgöwer, and M. A. Müller, *Data-based system*
481 *analysis and control of flat nonlinear systems*, in 2021 60th IEEE Conference on Decision and Control
482 (CDC), IEEE, 2021, pp. 1484–1489.
483 [3] D. A. Barton, *Control-based continuation: Bifurcation and stability analysis for physical experiments*,
484 Mechanical Systems and Signal Processing, 84 (2017), pp. 54–64.
485 [4] D. A. Barton, B. P. Mann, and S. G. Burrow, *Control-based continuation for investigating nonlinear*
486 *experiments*, Journal of Vibration and Control, 18 (2012), pp. 509–520.
487 [5] D. A. Barton and J. Sieber, *Systematic experimental exploration of bifurcations with noninvasive*
488 *control*, Physical Review E—Statistical, Nonlinear, and Soft Matter Physics, 87 (2013), p. 052916.
489 [6] J. Berberich and F. Allgöwer, *A trajectory-based framework for data-driven system analysis and*
490 *control*, in 2020 European Control Conference (ECC), IEEE, 2020, pp. 1365–1370.
491 [7] J. Berberich, J. Köhler, M. A. Müller, and F. Allgöwer, *Data-driven model predictive control:*
492 *closed-loop guarantees and experimental results*, at-Automatisierungstechnik, 69 (2021), pp. 608–618.
493 [8] L. Böttcher, H. Wallner, N. Kruse, W. Just, I. Barke, J. Starke, and S. Speller, *Exposing*
494 *hidden periodic orbits in scanning force microscopy*, Communications Physics, 8 (2025), pp. 1–9.
495 [9] J. J. Bramburger, J. N. Kutz, and S. L. Brunton, *Data-driven stabilization of periodic orbits*, IEEE
496 Access, 9 (2021), pp. 43504–43521.
497 [10] E. Bureau, F. Schilder, M. Elmegård, I. F. Santos, J. J. Thomsen, and J. Starke, *Experimental*
498 *bifurcation analysis of an impact oscillator—determining stability*, Journal of Sound and Vibration,
499 333 (2014), pp. 5464–5474.
500 [11] E. Bureau, F. Schilder, I. F. Santos, J. J. Thomsen, and J. Starke, *Experimental bifurcation*
501 *analysis of an impact oscillator—tuning a non-invasive control scheme*, Journal of Sound and Vibra-
502 tion, 332 (2013), pp. 5883–5897.
503 [12] C. Chen, *Linear System Theory and Design*, Oxford series in electrical and computer engineering, Oxford
504 University Press, 2013.
505 [13] C. De Persis, M. Rotulo, and P. Tesi, *Learning controllers from data via approximate nonlinearity*
506 *cancellation*, IEEE Transactions on Automatic Control, 68 (2023), pp. 6082–6097.
507 [14] C. De Persis and P. Tesi, *Formulas for data-driven control: Stabilization, optimality, and robustness*,
508 IEEE Transactions on Automatic Control, 65 (2019), pp. 909–924.
509 [15] A. Dittus, N. Kruse, I. Barke, S. Speller, and J. Starke, *Detecting stability and bifurcation points*
510 *in control-based continuation for a physical experiment of the zeeman catastrophe machine*, SIAM
511 Journal on Applied Dynamical Systems, 22 (2023), pp. 1275–1299.
512 [16] A. Dittus, N. Kruse, H. Wallner, L. Böttcher, I. Barke, S. Speller, J. Starke, and W. Just,
513 *Stroboscopic control and tracking of periodic states*, Nonlinear Dynamics, 112 (2024), pp. 1261–1274.
514 [17] M. Grant and S. Boyd, *Graph implementations for nonsmooth convex programs*, in Recent Advances
515 in Learning and Control, V. Blondel, S. Boyd, and H. Kimura, eds., Lecture Notes in Control and
516 Information Sciences, Springer-Verlag Limited, 2008, pp. 95–110. http://stanford.edu/~boyd/graph_
517 dcp.html.
518 [18] M. Grant and S. Boyd, *CVX: Matlab software for disciplined convex programming, version 2.1*. https:
519 //cvxr.com/cvx, Mar. 2014.
520 [19] J. Guckenheimer and P. Holmes, *Nonlinear oscillations, dynamical systems, and bifurcations of vector*
521 *fields*, vol. 42, Springer Science & Business Media, 2013.
522 [20] P. Holmes, *A nonlinear oscillator with a strange attractor*, Philosophical Transactions of the Royal
523 Society of London. Series A, Mathematical and Physical Sciences, 292 (1979), pp. 419–448.
524 [21] A. Hübler and E. Lüscher, *Resonant stimulation and control of nonlinear oscillators*, Naturwis-
525 senschaften, 76 (1989), pp. 67–69.
526 [22] A. Isidori, *Nonlinear Control Systems*, Communications and Control Engineering, Springer London,

1995.
[23] H. K. Khalil, *Nonlinear systems*, Prentice Hall, Upper Saddle River, N.J., 2002.
[24] M. Korda and I. Mezić, *Linear predictors for nonlinear dynamical systems: Koopman operator meets model predictive control*, Automatica, 93 (2018), pp. 149–160.
[25] N. Kruse, H. Wallner, A. Dittus, L. Böttcher, I. Barke, S. Speller, J. Starke, and W. Just, *Large basins of attraction for control-based continuation of unstable periodic states*, Nonlinear Dynamics, 112 (2024), pp. 19809–19823.
[26] K. Ogata, *Discrete-Time Control Systems*, Prentice Hall, Australia, Sydney, 1987.
[27] E. Ott, C. Grebogi, and J. A. Yorke, *Controlling chaos*, Phys. Rev. Lett., 64 (1990), pp. 1196–1199, https://doi.org/10.1103/PhysRevLett.64.1196.
[28] N. H. Packard, J. P. Crutchfield, J. D. Farmer, and R. S. Shaw, *Geometry from a time series*, Physical review letters, 45 (1980), p. 712.
[29] I. Panagiotopoulos, J. Starke, and W. Just, *Control of collective human behavior: Social dynamics beyond modeling*, Physical Review Research, 4 (2022), p. 043190.
[30] I. Panagiotopoulos, J. Starke, and W. Just, *Control of collective human behavior: Social dynamics beyond modeling*, Physical Review Research, 4 (2022), p. 043190.
[31] I. Panagiotopoulos, J. Starke, J. Sieber, and W. Just, *Continuation with noninvasive control schemes: Revealing unstable states in a pedestrian evacuation scenario*, SIAM Journal on Applied Dynamical Systems, 22 (2023), pp. 1–36.
[32] J. L. Proctor, S. L. Brunton, and J. N. Kutz, *Dynamic mode decomposition with control*, SIAM Journal on Applied Dynamical Systems, 15 (2016), pp. 142–161.
[33] L. Renson, A. Gonzalez-Buelga, D. A. Barton, and S. A. Neild, *Robust identification of backbone curves using control-based continuation*, Journal of Sound and Vibration, 367 (2016), pp. 145–158.
[34] C. Scherer and S. Weiland, *Linear matrix inequalities in control*, Lecture Notes, Dutch Institute for Systems and Control, Delft, The Netherlands, 3 (2000).
[35] F. Schilder, E. Bureau, I. F. Santos, J. J. Thomsen, and J. Starke, *Experimental bifurcation analysis—continuation for noise-contaminated zero problems*, Journal of Sound and Vibration, 358 (2015), pp. 251–266.
[36] J. Sieber and B. Krauskopf, *Control based bifurcation analysis for experiments*, Nonlinear Dynamics, 51 (2008), pp. 365–377.
[37] J. Sieber, B. Krauskopf, D. Wagg, S. Neild, and A. Gonzalez-Buelga, *Control-based continuation of unstable periodic orbits*, Journal of Computational and Nonlinear Dynamics, 6 (2010), p. 011005, https://doi.org/10.1115/1.4002101.
[38] C. I. Siettos, I. G. Kevrekidis, and D. Maroudas, *Coarse bifurcation diagrams via microscopic simulators: a state-feedback control-based approach*, International Journal of Bifurcation and Chaos, 14 (2004), pp. 207–220.
[39] F. Takens, *Detecting strange attractors in turbulence*, in Dynamical Systems and Turbulence, Warwick 1980: proceedings of a symposium held at the University of Warwick 1979/80, Springer, 2006, pp. 366–381.